Physics Letters B 763 (2016) 341–346

Contents lists available at ScienceDirect

Physics Letters B

www.elsevier.com/locate/physletb

Determination of the top-quark mass from hadro-production of single top-quarks

S. Alekhin [a,b], S. Moch [a,*], S. Thier [a]

[a] II. Institut für Theoretische Physik, Universität Hamburg, Luruper Chaussee 149, D-22761 Hamburg, Germany
[b] Institute for High Energy Physics, 142281 Protvino, Moscow region, Russia

ARTICLE INFO

Article history:
Received 30 August 2016
Received in revised form 15 October 2016
Accepted 20 October 2016
Available online 28 October 2016
Editor: A. Ringwald

ABSTRACT

We present a new determination of the top-quark mass m_t based on the experimental data from the Tevatron and the LHC for single-top hadro-production. We use the inclusive cross sections of s- and t-channel top-quark production to extract m_t and to minimize the dependence on the strong coupling constant and the gluon distribution in the proton compared to the hadro-production of top-quark pairs. As part of our analysis we compute the next-to-next-to-leading order approximation for the s-channel cross section in perturbative QCD based on the known soft-gluon corrections and implement it in the program HatHor for the numerical evaluation of the hadronic cross section. Results for the top-quark mass are reported in the $\overline{\text{MS}}$ and in the on-shell renormalization scheme.

Since the discovery of the top-quark in 1995 [1,2], the precise value of its mass has always been of great interest as a fundamental parameter of the Standard Model (SM). In the course of time several approaches have been used to extract the top-quark mass m_t as summarized for instance in [3]. While kinematic fits to the top-quark decay products allow for a very precise determination of parameters in Monte Carlo (MC) programs that are used to describe the measured distributions, the relation of these MC parameters to the fundamental SM parameters needs to be calibrated and related uncertainties need to be taken into account [4]. The determination of the top-quark mass from inclusive cross sections measured at the hadron colliders Tevatron and the Large Hadron Collider (LHC) provides an alternative way. This allows to relate the experimental cross section measurements directly to theoretical calculations which use a top-quark mass parameter in a well-defined renormalization scheme.

In this regard, the pair production of top-quarks has been of primary interest. It is dominantly mediated by the strong interactions. In consequence, theoretical predictions for top-quark pair production are highly sensitive to the value of the strong coupling constant α_s as well as to the parton luminosity parameterized through the parton distribution functions (PDFs) of the colliding hadrons. In fact, the uncertainty in the value of α_s and the dependence on the gluon PDF are the dominant sources which limit the precision of current theory predictions at the LHC [5]. Future measurements in particular at the LHC in Run 2 can potentially provide improved determinations of α_s and the PDFs, yet it is worth to investigate other methods to access m_t that do not rely on these controversial quantities.

In this letter we determine the top-quark mass based on single-top production cross section measurements as a complementary way to arrive at a well-defined value for m_t that is largely independent of α_s and the gluon PDFs. Single-top production generates the top-quark in an electroweak interaction, predominantly in a vertex with a bottom-quark and a W-boson. The orientation of this vertex assigns single-top production diagrams to different channels as illustrated in Fig. 1. As our focus is on the minimization of the correlation between m_t, α_s and the gluon luminosity, we consider only the so-called s-channel and t-channel production of single top-quarks in the following. The cross sections for those processes are directly proportional to the light quark PDFs, which are nowadays well constrained by data on the measured charged lepton asymmetries from $W^{\pm}$ gauge-boson production at the LHC. We use the inclusive single-top cross section measurements for those channels to determine m_t and compare the results to the ones obtained from $t\bar{t}$ production. Our study is based on data from the Tevatron at center-of-mass energy $\sqrt{S} = 1.96$ TeV as well as from the LHC at $\sqrt{S} = 7, 8$ and the most recent one at 13 TeV.

The theoretical description of both top-quark pair production and single-top production has reached a very high level of accuracy. The total cross section of $t\bar{t}$ hadro-production has been calculated up to the next-to-next-to-leading order (NNLO) corrections

* Corresponding author.
E-mail address: sven-olaf.moch@desy.de (S. Moch).

http://dx.doi.org/10.1016/j.physletb.2016.10.062

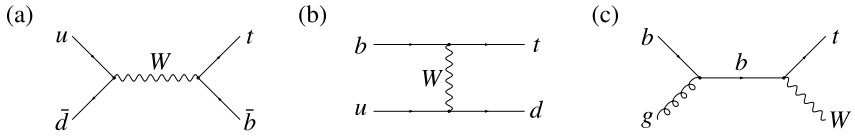

Fig. 1. Representative leading order Feynman diagrams for single top-quark production: (a) s-channel; (b) t-channel; (c) in association with a W boson.

in perturbative QCD [6–9]. The NNLO result shows good apparent convergence of the perturbative expansion and greatly reduced sensitivity with respect to a variation of the renormalization and factorization scales μ_R and μ_F, which is conventionally taken to estimate the uncertainty from the truncation of the perturbation series.

For the t-channel of single-top production, the NNLO QCD corrections have been determined in the structure function approximation [10] (see also Ref. [11]), by computing separately the QCD corrections to the light- and heavy-quark lines, see Fig. 1 (b). Any dynamical cross-talk between the two quark lines, e.g., double-box topologies, has been neglected in Ref. [10] and is expected to be small due to color suppression. The current theoretical status regarding those non-factorizing corrections is summarized in Ref. [12].

The inclusive cross section of s-channel single-top production is fully known up to the next-to-leading order (NLO) QCD corrections [13], see also [14] for fully differential results. Beyond NLO accuracy, fixed-order expansions of the resummed soft-gluon contributions up to the next-to-leading logarithms (NLL) have been provided as an approximation of the complete NNLO result, both for the Tevatron [15] and the LHC [16]. Subsequently, these results have been extended to next-to-next-to-leading logarithmic (NNLL) accuracy [17]. The threshold corrections in the s-channel are large and dominant and, therefore, they provide a good approximation to the full exact result, see Ref. [18] for a validation at NLO. In our study we use Refs. [15–17] to derive compact expressions for the approximate corrections at NLO and NNLO including soft-gluon effects almost complete to NNLL accuracy. To that end, we integrate the partonic double-differential cross section given in Refs. [15–17] over the phase space, i.e., the partonic Mandelstam variables t and u, and obtain the inclusive partonic cross section to logarithmic accuracy in the top-quark velocity $\beta = (1 - m_t^2/s)^{1/2}$.

We expand the partonic cross section for s-channel single-top production as a power series

$$\sigma = \sigma^{(0)} + \alpha_s \sigma^{(1)} + \alpha_s^2 \sigma^{(2)}, \tag{1}$$

with $\alpha_s = \alpha_s(\mu_R)$ taken at the renormalization scale μ_R and the leading-order partonic cross section for the process $u\bar{d} \to t\bar{b}$ given by

$$\sigma^{(0)} = \frac{\pi \alpha^2 V_{tb}^2 V_{ud}^2 (m_t^2 - s)^2 (m_t^2 + 2s)}{24 s^2 \sin^4\theta_W (m_W^2 - s)^2}. \tag{2}$$

Here, $\sqrt{s}$ is the partonic center-of-mass energy, m_W the W-boson mass and α, $\sin\theta_W$, V_{tb} and V_{ud} are the electroweak and CKM parameters [19].

The NLO result in Eq. (1) is denoted $\sigma^{(1)}$ and the exact result is known [13] and has been implemented in the program HatHor [20,19] for a fast and efficient evaluation of the total cross section. Based on the threshold enhanced soft-gluon contributions we can provide an approximate NLO (aNLO) result for $\sigma^{(1)}$ as

$$\sigma^{(1)} \simeq \sigma^{(0)} \left(1 - \beta^2\right) \frac{C_F}{8\pi} \left(112 \log^2(\beta) - 148 \log(\beta) + 63 - 4 \log\left(\frac{\mu_F^2}{m_t^2}\right) (8 \log(\beta) - 3) \right) + \mathcal{O}(\beta), \tag{3}$$

where the coefficients of $\log^2(\beta)$ and $\log(\beta)$ are exact while we are lacking terms independent of β, i.e., $\mathcal{O}(\beta^0)$ from the virtual contributions at one loop. In addition we multiply the result by a kinematical suppression factor $(1 - \beta^2) = m_t^2/s$ to restrict the soft-gluon logarithms to the threshold region.

The NNLO result $\sigma^{(2)}$ in Eq. (1) is currently unknown, but we can compute an approximate NNLO (aNNLO) expression for $\sigma^{(2)}$ valid near threshold $\beta \simeq 0$ as

$$\begin{aligned}
\sigma^{(2)} \simeq \sigma^{(0)} \left(1 - \beta^2\right) \frac{C_F}{24\pi^2} \Bigg(& 2352 C_F \log^4(\beta) \\
& - 8 \log^3(\beta)(17\beta_0 + 777 C_F) \\
& + \frac{1}{3} \log^2(\beta) \left(801\beta_0 - 28\left(3\pi^2 - 67\right) C_A + 24759 C_F \right. \\
& \left. - 504\pi^2 C_F - 280 n_f + \frac{144}{N_c} \right) \\
& + \frac{1}{18} \log(\beta) \left(-4293\beta_0 + C_A \left(3240\zeta_3 - 18007 + 1008\pi^2 \right) \right. \\
& + 6480 C_F \zeta_3 - 111348 C_F + 4104\pi^2 C_F + 2758 n_f \\
& \left. - 72\pi^2 n_f + \frac{3456}{N_c}\zeta_3 + \frac{288}{N_c}\pi^2 - \frac{7344}{N_c} \right) \\
& - \frac{1}{120} \left(-10215\beta_0 + 25 C_A \left(648\zeta_3 - 2315 + 144\pi^2 \right) \right. \\
& + 32400 C_F \zeta_3 - 251550 C_F + 11880\pi^2 C_F + 8990 n_f \\
& \left. - 360\pi^2 n_f + \frac{23040}{N_c}\zeta_3 + \frac{32}{N_c}\pi^4 + \frac{3840}{N_c}\pi^2 - \frac{69120}{N_c} \right) \\
& + \log\left(\frac{\mu_F^2}{m_t^2}\right) \left(-1344 C_F \log^3(\beta) \right. \\
& + 12 \log^2(\beta)(7\beta_0 + 190 C_F) - \frac{1}{3}\log(\beta)\left(333\beta_0 \right. \\
& \left. - 8\left(3\pi^2 - 67\right) C_A + 6066 C_F - 144\pi^2 C_F - 80 n_f \right) \\
& + \frac{1}{4}\left(189\beta_0 - 8\left(3\pi^2 - 67\right) C_A + 3282 C_F - 144\pi^2 C_F \right. \\
& \left. \left. - 80 n_f \right) + \log\left(\frac{\mu_R^2}{\mu_F^2}\right) \left(-24\beta_0 \log(\beta) + 18\beta_0 \right) \right) \\
& + \log^2\left(\frac{\mu_F^2}{m_t^2}\right) \left(192 C_F \log^2(\beta) - 12 \log(\beta)(\beta_0 + 12 C_F) \right. \\
& \left. + 3(3\beta_0 + 20 C_F) \right) + \log\left(\frac{\mu_R^2}{\mu_F^2}\right) \left(84\beta_0 \log^2(\beta) \right. \\
& \left. \left. - 111\beta_0 \log(\beta) + \frac{189}{4}\beta_0 \right) \right) + \mathcal{O}(\beta)
\end{aligned} \tag{4}$$

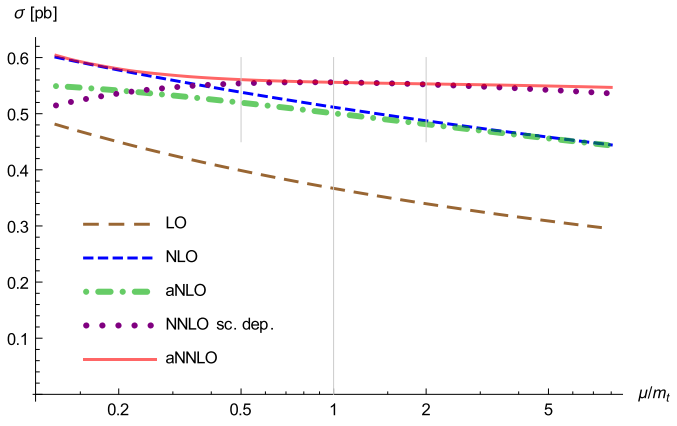

Fig. 2. Cross section of single-top production in the s-channel for $p\bar{p}$ collisions using $\sqrt{S} = 1.96$ TeV, $m_t^{\text{pole}} = 172.5$ GeV and the ABM12 PDFs [21] as function of μ/m_t with $\mu = \mu_R = \mu_F$ at LO (brown, long-dashed), at NLO (blue, short-dashed), at aNLO (green, dashed–dotted), at aNNLO (red, solid), and with scale dependence exact at NNLO (purple, dotted). The vertical lines indicate the nominal scale $\mu = m_t$ and the conventional range $1/2 \leq \mu/m_t \leq 2$ for the variation.

where $\beta_0 = (11C_A - 2n_f)/3$ and n_f is the number of quark flavors. Moreover, we have $C_F = 4/3$ and $C_A = 3$ in QCD with $N_c = 3$ colors and ζ_3 denotes the Riemann ζ-function.

In Eq. (4) all terms proportional to $\log^4(\beta)$ and $\log^3(\beta)$ are exact while those starting from $\log^2(\beta)$ are complete up to the interference of the one-loop threshold logarithms in Eq. (3) with the $\mathcal{O}(\beta^0)$ part of the one-loop virtual corrections. In our subsequent phenomenological studies we therefore restrict the use of threshold logarithms in Eq. (4). For the scale independent part we keep all terms proportional to $\log^k(\beta)$ with $k = 4, 3, 2$. In analogy, we also keep the first three terms of the threshold expansion in Eq. (4) for all parts proportional to logarithms of μ_R or μ_F, that is $\log(\mu)\log^k(\beta)$ with $k = 3, 2, 1$ and $\log^2(\mu)\log^k(\beta)$ with $k = 2, 1, 0$. In this way, we define the partonic cross section in the s-channel at approximate NNLO accuracy.

As a check of the convergence and the perturbative stability we show the scale dependence in Fig. 2 at LO, NLO and NNLO for $p\bar{p}$ collisions at $\sqrt{S} = 1.96$ TeV. We focus here mainly on Tevatron kinematics for s-channel single-top production, since this process has not yet been established as an accurate enough observation at the LHC. We use a pole mass $m_t^{\text{pole}} = 172.5$ GeV, the PDFs of the ABM12 set [21] and we identify $\mu = \mu_R = \mu_F$. At NLO we plot the exact result [13] and compare to the threshold approximation for $\sigma^{(1)}$ given in Eq. (3) and show that it approximates the exact result very well. In fact, around the nominal scale $\mu = m_t$ the deviations of the aNLO result Eq. (3) from the exact one typically amount to only 5% or less for collider energies in the range $\sqrt{S} = 1$ to 5 TeV. At NNLO, we use the result for $\sigma^{(2)}$ in Eq. (4) including the scale dependent terms and subject to the truncation discussed above. As an alternative, instead of those scale logarithms we can use the exact scale dependence at NNLO, which is provided by the program HatHor in numerical form, see [19]. Again, the differences between the two results are small except for very small values of μ. In this case, numerically large but power suppressed contributions $\mathcal{O}(\beta)$ in the scale dependent part cause variations which remain uncanceled by the scale independent terms in Eq. (4). In the conventionally chosen range $1/2 \leq \mu/m_t \leq 2$ for the scale variations indicated by the vertical lines in Fig. 2 any differences in the methodology to estimate the NNLO corrections are small so that we consider Eq. (4) restricted to the first three terms of the threshold expansion to provide a reliable approximation for the NNLO term $\sigma^{(2)}$ in Eq. (1). Below, we will use the residual scale dependence to estimate both the error due to the truncation of the perturbative expansion in Eq. (1) as well as the systematic uncertainty inherent in the threshold approximation defining our aNNLO result. See also Ref. [18] for a further discussion of the validation of our approximation method.

The theoretical calculations for the hadro-production of top-quarks, singly or in pairs, typically use the on-shell renormalization scheme for the top-quark so that the cross section predictions are given in terms of the pole mass m_t^{pole}. The advantages of other renormalization schemes which implement so-called short-distance masses, like the $\overline{\text{MS}}$ mass $m_t(\mu)$ at the scale μ, have been discussed in the literature at length, see for instance [22,23,4]. The relation between the on-shell mass m_t^{pole} and the $\overline{\text{MS}}$ mass is known up to four loops in perturbation theory [24,25] and can be used to convert the respective cross sections. See for instance Refs. [23,20] for the derivation of $\sigma(m_t(m_t))$ in terms of the $\overline{\text{MS}}$ mass $m_t(m_t)$ at $\mu = m_t$ from $\sigma(m_t^{\text{pole}})$. In summary, cross sections for the hadro-production of top-quark pairs exhibit a faster convergence and better scale stability if expressed in terms of the $\overline{\text{MS}}$ mass.

This improved convergence is also observed for single-top production in the s-channel. Evaluating the cross section for s-channel single-top production in $p\bar{p}$ collisions at $\sqrt{S} = 1.96$ TeV with the ABM12 PDFs and $m_t^{\text{pole}} = 172.5$ GeV, we find $\sigma_{\text{LO}} = 0.37$ pb, $\sigma_{\text{NLO}} = 0.51$ pb, and $\sigma_{\text{aNNLO}} = 0.56$ pb, which corresponds to an increase of 39% at NLO relative to LO and an increase of 9% at aNNLO relative to NLO. This growth is reduced when the cross section is calculated for $m_t(m_t) = 163.0$ GeV. In this case, we find the cross section values $\sigma_{\text{LO}} = 0.47$ pb, $\sigma_{\text{NLO}} = 0.57$ pb, and $\sigma_{\text{aNNLO}} = 0.58$ pb with an increase of 20% at NLO relative to LO and an increase of 3% at aNNLO relative to NLO.

For the independent variation of both the renormalization scale μ_R and the factorization scale μ_F between $\frac{1}{2}m_t$ and $2m_t$, excluding the points where both scales are shifted in opposite directions, we see some increase in stability when using the $\overline{\text{MS}}$ mass. In $p\bar{p}$ collisions at $\sqrt{S} = 1.96$ TeV we find for a pole mass of 172.5 GeV variations relative to the cross section at the central scale m_t of $+5.2\%/-4.7\%$ at NLO and $+2.8\%/-2.4\%$ at aNNLO. When the cross section is expressed as function of the $\overline{\text{MS}}$ mass, which we set to 163 GeV here, the scale dependence at NLO is reduced to $+3.1\%/-3.2\%$. The scale dependence at aNNLO is $+3.6\%/-2.7\%$ for $m_t(m_t)$, similar to though slightly larger than the scale dependence in the case of the pole mass. The range of variations can be considered as an inherent uncertainty of our approximation for Tevatron collisions. At higher energies, like in pp collisions at the LHC with $\sqrt{S} = 8$ TeV, the threshold approximation is less accurate and we find scale uncertainties of $+5.3\%/-4.4\%$ and $+6.4\%/-5.3\%$ at aNNLO for the pole mass and the $\overline{\text{MS}}$ mass respectively.

Due to the pattern of improved convergence observed in all production processes, we use the $\overline{\text{MS}}$ scheme in our determination of the top-quark mass. The fits to measured data are performed with the program HatHor [20,19], which computes the inclusive cross sections for $t\bar{t}$ and single-top production. In the s-channel, we implement our aNNLO result Eq. (4) for the partonic cross section in HatHor and combine it with the built-in NLO formulae. To evaluate the t-channel total cross section, we use the NLO QCD predictions included in HatHor and rescale them to account for the small NNLO QCD corrections calculated in Ref. [10]. In our analysis we use a common factor $k = 0.984$ for the t and $\bar{t}$ final states alike for this rescaling. This is justified as follows.

For the t-channel total cross section for a single t-quark Ref. [10] reports a reduction by -1.6% at NNLO compared to NLO and for the one for a single $\bar{t}$-quark by -1.3%, respectively. Hence, there exists a slight dependence on the final state (see Tabs. 1 and 2 in Ref. [10]). It is worth pointing out, though, that the num-

Table 1
The data on single-top production in association with a light quark q or $\bar{b}$-quark from the LHC and Tevatron used in the present analysis. The errors given are combinations of the statistical, systematical, and luminosity ones.

Experiment	ATLAS			CMS			CDF & D0
$\sqrt{S}$ (TeV)	7	8	13	7	8	13	1.96
Final states	tq	tq	tq	tq	tq	tq	$tq, t\bar{b}$
Reference	[26]	[27]	[28]	[29]	[30]	[31]	[32]
Luminosity (1/fb)	4.59	20.3	3.2	2.73	19.7	2.3	9.7x2
Cross section (pb)	68 ± 8	82.6 ± 12.1	247 ± 46	67.2 ± 6.1	83.6 ± 7.7	232 ± 31	$3.30^{+0.52}_{-0.40}$ (sum)

Table 2
The data on the $t\bar{t}$-production cross section from the LHC used in the present analysis. The errors given are combinations of the statistical and systematical ones. An additional error of 3.3, 4.2 and 12 pb due to the beam energy uncertainty applies to all entries for the collision energy of $\sqrt{S} = 7, 8$ and 13 TeV, respectively. The quoted values are rounded for the purpose of a compact presentation.

		Cross section (pb)					
$\sqrt{S}$ (TeV)		7		8		13	
Experiment		ATLAS	CMS	ATLAS	CMS	ATLAS	CMS
Decay mode	dilepton + jets	181 ± 11 [33]	174 ± 6 [34]		245 ± 9 [34]		746 ± 86 [35]
	dilepton + b-jet(s)	183 ± 6 [36]		242 ± 9 [36]		818 ± 36 [37]	793 ± 44 [38]
	lepton + jets		162 ± 14 [39]	260 ± 24 [40]	229 ± 15 [39]		836 ± 133 [41]
	lepton + jets, $b \to \mu\ \nu\ X$	165 ± 17 [42]					
	lepton + $\tau \to$ hadrons	183 ± 25 [43]	143 ± 26 [44]		257 ± 25 [45]		
	jets + $\tau \to$ hadrons	194 ± 49 [46]	152 ± 34 [47]				
	all-jets	168 ± 60 [48]	139 ± 28 [49]		276 ± 39 [50]		834^{+123}_{-109} [51]

Table 3
Results for the running mass $m_t(m_t)$ in the $\overline{\text{MS}}$ scheme from the data listed in Tables 1 and 2 using different PDFs.

Channel	ABM12 [21]	ABMP15 [52]	CT14 [55]	MMHT14 [56]	NNPDF3.0 [57]
$t\bar{t}$	158.6 ± 0.6	158.4 ± 0.6	164.7 ± 0.6	164.6 ± 0.6	164.3 ± 0.6
t-channel	158.7 ± 3.7	158.0 ± 3.7	160.1 ± 3.8	160.5 ± 3.8	164.0 ± 3.8
s- & t-channel	158.4 ± 3.3	157.7 ± 3.3	159.1 ± 3.4	159.6 ± 3.4	162.4 ± 3.5

bers reported in Ref. [10] implicitly depend on the perturbative accuracy of the chosen PDF sets as they have been obtained with a consistent use of PDFs, i.e. NLO (NNLO) PDFs for NLO (NNLO) predictions. If we use NNLO PDF sets uniformly at every order for the cases considered in Ref. [10] we find a reduction of the cross section by -1.2% at NNLO compared to NLO, independent of the final state. This illustrates the limitations in accuracy of the rescaling method being at the level of a few per mill for the t-channel total cross section, which is acceptable because any possible PDF dependence is small compared to the still sizable experimental uncertainties.

The cross section measurements of single-top production at the Tevatron and at the LHC that we use for our analysis are displayed in Table 1. For s-channel single-top production only Tevatron data are available. In the t-channel, we combine Tevatron data with the LHC ones at $\sqrt{S} = 7$, 8 and 13 TeV. When a separation of t and $\bar{t}$ final states is provided [26,30,28,31], we employ this information in our analysis. In this case a correlation between the systematic uncertainties in the single t- and $\bar{t}$-production data are taken into account using the error correlation coefficients

$$C_{t,\bar{t}} = \left(\delta\sigma_{t+\bar{t}}\right)^2 - \left(\delta\sigma_t\right)^2 - \left(\delta\sigma_{\bar{t}}\right)^2 , \tag{5}$$

where $\delta\sigma_t$, $\delta\sigma_{\bar{t}}$, and $\delta\sigma_{t+\bar{t}}$ are the systematic errors in the measured cross sections for the final states containing a single t-quark, a $\bar{t}$-quark, and either t or $\bar{t}$, respectively. The impact of the systematics correlation encoded in Eq. (5) turns out to be more pronounced for the data samples of Refs. [30,28] and it is marginal for the ones of Refs. [26,31]. Here, the luminosity errors quoted in Refs. [28,31] are taken as fully correlated between the separated final states.

We extract the t-quark mass also from data on $t\bar{t}$-production for comparison. All inclusive cross sections obtained at the LHC at $\sqrt{S} = 7$, 8, and 13 TeV are summarized in Table 2. These samples are categorized by the t-quark decay channels containing different numbers of the final-state leptons and jets. The systematic uncertainties in different channels and energies are taken as uncorrelated in general, however, the errors due to beam energy and luminosity are correlated for the data collected at the same collision energy. In addition to the data listed in Table 2 we also employ a combination of the measurements in different channels performed at Tevatron [53] and the recent CMS data [54] for the $e\mu$ decay channel at $\sqrt{S} = 5$ TeV.

Our results for $m_t(m_t)$ from the fit to single-top cross sections using the different modern PDF sets ABM12 [21], ABMP15 [52], CT14 [55], MMHT14 [56], and NNPDF3.0 [57] are collected in Table 3 together with corresponding mass values that are derived with the help of the $t\bar{t}$ cross section data. The uncertainties in Table 3 correspond to the ones which were reported by the experiments for the respective data. In addition, there are theoretical uncertainties Δm_t from the variation of the factorization and renormalization scales in the usual range $\frac{1}{2} m_t(m_t) \le \mu \le 2 m_t(m_t)$ for $\mu = \mu_R = \mu_F$. These are small and process dependent, but otherwise largely independent of the precise numerical value of the top-quark mass or of the specific PDF set considered in Table 3. We can quantify the effect of the scale variation on the extracted top-quark mass in the $\overline{\text{MS}}$ scheme as $\Delta m_t = \pm 0.7$ GeV for the $t\bar{t}$ total cross section, see e.g. [21]. Fits of the $\overline{\text{MS}}$ mass to Tevatron cross section data [58] for the respective scale choices show mass uncertainties of $\Delta m_t = +0.9/-1.0$ GeV when our aNNLO approximation is used in the s-channel. In that case we have to account for an additional $\Delta m_t = \pm 1.0$ GeV from the systematics of the threshold approximation used to define the aNNLO s-channel result. The latter estimate is based on the accuracy of the threshold approximation at NLO, i.e., the difference for the cross sections at the scale $\mu = m_t$ obtained either at NLO or at aNLO, cf. Fig. 2. For

Table 4
Results for $m_t^{\rm pole}$ for different PDFs from the conversion of $m_t(m_t)$ at NNLO (in parenthesis at N^{3}LO) using the value of $\alpha_s(m_Z)$ corresponding to the respective PDF set.

Channel	ABM12 [21]	ABMP15 [52]	CT14 [55]	MMHT14 [56]	NNPDF3.0 [57]
$t\bar{t}$	167.3 ± 0.6 (167.9 ± 0.6)	167.1 ± 0.6 (167.6 ± 0.6)	174.1 ± 0.6 (174.7 ± 0.6)	174.0 ± 0.6 (174.6 ± 0.6)	173.7 ± 0.6 (174.3 ± 0.6)
t-channel	167.4 ± 3.9 (168.0 ± 3.9)	166.7 ± 3.9 (167.2 ± 3.9)	169.3 ± 4.0 (169.9 ± 4.0)	169.7 ± 4.0 (170.3 ± 4.0)	173.4 ± 4.0 (174.0 ± 4.0)
s- & t-channel	167.1 ± 3.5 (167.6 ± 3.5)	166.4 ± 3.5 (166.9 ± 3.5)	168.2 ± 3.6 (168.8 ± 3.6)	168.7 ± 3.6 (169.4 ± 3.6)	171.7 ± 3.7 (172.3 ± 3.7)

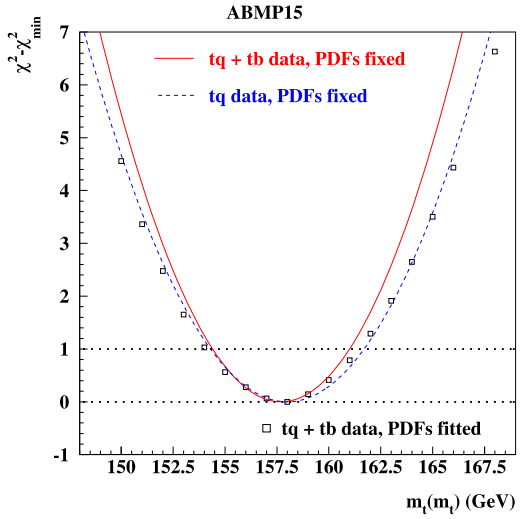

Fig. 3. A profile of χ^2 in a scan over the top-quark $\overline{\rm MS}$ mass obtained in the present analysis taking the ABMP15 PDFs [52] and the single-top production data (solid: combination of the s-channel and t-channel samples, dashes: t-channel sample only) in comparison with the results obtained in the variant of the ABMP15 fit with the s-channel and t-channel single-top data appended (squares). The minimal value $\chi^2_{\rm min} \sim 5$ is subtracted in all cases.

the t-channel, we determine mass variations at NLO accuracy in fits to the cross section data that were reported in [32] and subsequently take the reduced scale dependence into account that was found at NNLO [10]. In this way, we arrive at an uncertainty estimate of $\Delta m_t = +0.6/-0.5$ GeV for our result in the t-channel.

Due to the higher abundance of experimental data in the t-channel, we report results of the mass fit to either t-channel data alone or the combination of all considered single-top data in s- and t-channel. The inclusion of the s-channel data favors a slightly smaller mass value compared to the fit based on t-channel data alone, cf. also the χ^2 plot in Fig. 3.

In order to facilitate the comparison of our results for the top-quark mass to other studies of m_t, for instance an earlier analysis performed in Ref. [19], we provide a conversion of the $\overline{\rm MS}$ masses in Table 3 to the respective pole mass values in Table 4. The resulting pole mass $m_t^{\rm pole}$ in the second line is obtained from a scheme transformation to NNLO accuracy, using the program RunDec [59] and the value of $\alpha_s(m_Z)$ of the given PDF set.

Interestingly, the results in Tables 3 and 4 show a significant spread in the values of m_t obtained for the different PDF sets, but also when considering the different physical processes, i.e., the production of $t\bar{t}$-pairs versus single top-quarks in the s- and t-channel. For the PDF set ABM12 we obtain consistent values of $m_t(m_t)$ in Table 3, i.e., central values of $m_t(m_t) = 158.6$ GeV from the $t\bar{t}$ data and $m_t(m_t) = 158.4$ GeV from the combined s- and t-channel data. The results obtained for the ABMP15 set are very similar compared to those for ABM12. The ABMP15 PDFs are based on an improved determination of the up- and down-quarks in the proton with the help of recent data on charged lepton asymmetries from $W^\pm$ gauge-boson production at the LHC and Tevatron. In particular, the ABMP15 PDFs find a non-zero isospin asymmetry of the sea, $x(\bar{d} - \bar{u})$, at small values of Bjorken $x \simeq 10^{-4}$ and a delayed onset of the Regge asymptotics of a vanishing $x(\bar{d} - \bar{u})$-asymmetry at small-x. This affects to some extent the cross section for t-channel single-top production, but has overall little impact on the extracted value of $m_t(m_t)$ as can be seen from Table 3.

For the PDF sets CT14 and MMHT14 we find the central values $m_t(m_t) = 164.7$ GeV and $m_t(m_t) = 164.6$ GeV from the $t\bar{t}$ data. These are not only significantly larger than the ones obtained with ABM12 or ABMP15 due to the larger values for $\alpha_s(m_Z)$ and the gluon PDF in the relevant x-range [5], but also much bigger than and barely compatible with the corresponding ones extracted from data for the single-top cross sections, $m_t(m_t) = 159.1$ GeV and $m_t(m_t) = 159.6$ GeV. This lack of compatibility at the level of 1σ remains an issue even when considering both the still sizeable uncertainty on $m_t(m_t)$ from the precision of experimental data as listed in Table 3 and the theoretical uncertainty Δm_t due the scale variation discussed above. Finally, the $m_t(m_t)$ values determined with the NNPDF3.0 set are internally consistent yielding $m_t(m_t) = 164.3$ GeV and $m_t(m_t) = 162.4$ GeV, respectively, when using the $t\bar{t}$ data or the combined s- and t-channel data. However, they are significantly higher than the ones derived with the ABM12 and ABMP15 sets, so there is some tension among these two results. All the observed differences are directly translated to the on-shell masses listed in Table 4.

Our study has shown that already with currently available data the top-quark mass can be determined to good accuracy for single-top cross sections and in doing so we have chosen the $\overline{\rm MS}$ renormalization scheme for reasons of better perturbative stability. The values obtained for the combined s- and t-channel data can be used to perform internal consistency checks for a given PDF set when comparing with the ones from $t\bar{t}$ data. Based on the dominant soft-gluon corrections we have provided new approximate predictions at NNLO for the inclusive s-channel single-top cross section and future theory improvements should complete the NNLO QCD correction to this process. On the experimental side, high statistics measurements of single-top production at the LHC in Run 2 with $\sqrt{S} = 13$ TeV can help substantially to further improve the precision of the top-quark mass.

Acknowledgements

We would like to thank M. Aldaya Martin for discussions. This work has been supported by Deutsche Forschungsgemeinschaft in Sonderforschungsbereich SFB 676.

References

[1] F. Abe, et al., CDF, Phys. Rev. Lett. 74 (1995) 2626, arXiv:hep-ex/9503002.
[2] S. Abachi, et al., D0, Phys. Rev. Lett. 74 (1995) 2632, arXiv:hep-ex/9503003.
[3] K.A. Olive, et al., Particle Data Group, Chin. Phys. C 38 (2014) 090001.
[4] J. Kieseler, K. Lipka, S. Moch, Phys. Rev. Lett. 116 (16) (2016) 162001, arXiv:1511.00841.

[5] A. Accardi, et al., Eur. Phys. J. C 76 (8) (2016) 471, arXiv:1603.08906.
[6] P. Bärnreuther, M. Czakon, A. Mitov, Phys. Rev. Lett. 109 (2012) 132001, arXiv:1204.5201.
[7] M. Czakon, A. Mitov, J. High Energy Phys. 12 (2012) 054, arXiv:1207.0236.
[8] M. Czakon, A. Mitov, J. High Energy Phys. 01 (2013) 080, arXiv:1210.6832.
[9] M. Czakon, P. Fiedler, A. Mitov, Phys. Rev. Lett. 110 (2013) 252004, arXiv:1303.6254.
[10] M. Brucherseifer, F. Caola, K. Melnikov, Phys. Lett. B 736 (2014) 58, arXiv:1404.7116.
[11] E.L. Berger, J. Gao, C.P. Yuan, H.X. Zhu, arXiv:1606.08463, 2016.
[12] M. Assadsolimani, P. Kant, B. Tausk, P. Uwer, Phys. Rev. D 90 (11) (2014) 114024, arXiv:1409.3654.
[13] M.C. Smith, S. Willenbrock, Phys. Rev. D 54 (1996) 6696, arXiv:hep-ph/9604223.
[14] B.W. Harris, E. Laenen, L. Phaf, Z. Sullivan, S. Weinzierl, Phys. Rev. D 66 (2002) 054024, arXiv:hep-ph/0207055.
[15] N. Kidonakis, Phys. Rev. D 74 (2006) 114012, arXiv:hep-ph/0609287.
[16] N. Kidonakis, Phys. Rev. D 75 (2007) 071501, arXiv:hep-ph/0701080.
[17] N. Kidonakis, Phys. Rev. D 81 (2010) 054028, arXiv:1001.5034.
[18] S. Alekhin, S. Moch, S. Thier, arXiv:1607.00794, 2016.
[19] P. Kant, O.M. Kind, T. Kintscher, T. Lohse, T. Martini, S. Mölbitz, P. Rieck, P. Uwer, Comput. Phys. Commun. 191 (2015) 74, arXiv:1406.4403.
[20] M. Aliev, H. Lacker, U. Langenfeld, S. Moch, P. Uwer, M. Wiedermann, Comput. Phys. Commun. 182 (2011) 1034, arXiv:1007.1327.
[21] S. Alekhin, J. Blümlein, S. Moch, Phys. Rev. D 89 (5) (2014) 054028, arXiv:1310.3059.
[22] S. Fleming, A.H. Hoang, S. Mantry, I.W. Stewart, Phys. Rev. D 77 (2008) 114003, arXiv:0711.2079.
[23] U. Langenfeld, S. Moch, P. Uwer, Phys. Rev. D 80 (2009) 054009, arXiv:0906.5273.
[24] P. Marquard, A.V. Smirnov, V.A. Smirnov, M. Steinhauser, Phys. Rev. Lett. 114 (14) (2015) 142002, arXiv:1502.01030.
[25] P. Marquard, A.V. Smirnov, V.A. Smirnov, M. Steinhauser, D. Wellmann, arXiv:1606.06754, 2016.
[26] G. Aad, et al., ATLAS, Phys. Rev. D 90 (11) (2014) 112006, arXiv:1406.7844.
[27] P. Tepel, ATLAS, arXiv:1411.7627, 2014.
[28] M. Aaboud, et al., ATLAS, arXiv:1609.03920, 2016.
[29] S. Chatrchyan, et al., CMS, J. High Energy Phys. 12 (2012) 035, arXiv:1209.4533.
[30] V. Khachatryan, et al., CMS, J. High Energy Phys. 06 (2014) 090, arXiv:1403.7366.
[31] A.M. Sirunyan, et al., CMS, arXiv:1610.00678, 2016.
[32] T.A. Aaltonen, et al., CDF, D0, Phys. Rev. Lett. 115 (15) (2015) 152003, arXiv:1503.05027.
[33] G. Aad, et al., ATLAS, Phys. Rev. D 91 (5) (2015) 052005, arXiv:1407.0573.
[34] V. Khachatryan, et al., CMS, arXiv:1603.02303, 2016.
[35] V. Khachatryan, et al., CMS, Phys. Rev. Lett. 116 (5) (2016) 052002, arXiv:1510.05302.
[36] G. Aad, et al., ATLAS, Eur. Phys. J. C 74 (10) (2014) 3109, arXiv:1406.5375.
[37] M. Aaboud, et al., ATLAS, arXiv:1606.02699, 2016.
[38] Measurement of the top quark pair production cross section using eμ events in proton-proton collisions at $\sqrt{s} = 13$ TeV with the CMS detector, Tech. Rep. CMS-PAS-TOP-16-005, CERN, Geneva, 2016, https://cds.cern.ch/record/2141738.
[39] V. Khachatryan, et al., CMS, Eur. Phys. J. C (2016), in press, arXiv:1602.09024.
[40] G. Aad, et al., ATLAS, Phys. Rev. D 91 (11) (2015) 112013, arXiv:1504.04251.
[41] Measurement of the inclusive and differential tt production cross sections in lepton + jets final states at 13 TeV, Tech. Rep. CMS-PAS-TOP-15-005, CERN, Geneva, 2015, https://cds.cern.ch/record/2048622.
[42] Measurement of the top quark pair production cross-section with ATLAS in pp collisions at $\sqrt{s} = 7$ TeV in the single-lepton channel using semileptonic b decays, Tech. Rep. ATLAS-CONF-2012-131, CERN, Geneva, 2012, http://cds.cern.ch/record/1478370.
[43] G. Aad, et al., ATLAS, Phys. Rev. D 92 (7) (2015) 072005, arXiv:1506.05074.
[44] S. Chatrchyan, et al., CMS, Phys. Rev. D 85 (2012) 112007, arXiv:1203.6810.
[45] V. Khachatryan, et al., CMS, Phys. Lett. B 739 (2014) 23, arXiv:1407.6643.
[46] G. Aad, et al., ATLAS, Eur. Phys. J. C 73 (3) (2013) 2328, arXiv:1211.7205.
[47] S. Chatrchyan, et al., CMS, Eur. Phys. J. C 73 (4) (2013) 2386, arXiv:1301.5755.
[48] Measurement of the $t\bar{t}$ production cross section in the all-hadronic channel in ATLAS with $\sqrt{s} = 7$ TeV data, Tech. Rep. ATLAS-CONF-2012-031, CERN, Geneva, 2012, http://cds.cern.ch/record/1432196.
[49] S. Chatrchyan, et al., CMS, J. High Energy Phys. 05 (2013) 065, arXiv:1302.0508.
[50] V. Khachatryan, et al., CMS, Eur. Phys. J. C 76 (3) (2016) 128, arXiv:1509.06076.
[51] Measurement of the $t\bar{t}$ production cross section at 13 TeV in the all-jets final state, Tech. Rep. CMS-PAS-TOP-16-013, CERN, Geneva, 2016, https://cds.cern.ch/record/2161138.
[52] S. Alekhin, J. Blümlein, S. Moch, R. Placakyte, arXiv:1508.07923, 2015.
[53] T.A. Aaltonen, et al., CDF, D0, Phys. Rev. D 89 (7) (2014) 072001, arXiv:1309.7570.
[54] First measurement of the top quark pair production cross section in proton-proton collisions at $\sqrt{s} = 5.02$ TeV, Tech. Rep. CMS-PAS-TOP-16-015, CERN, Geneva, 2016, https://cds.cern.ch/record/2161499.
[55] S. Dulat, T.-J. Hou, J. Gao, M. Guzzi, J. Huston, P. Nadolsky, J. Pumplin, C. Schmidt, D. Stump, C.P. Yuan, Phys. Rev. D 93 (3) (2016) 033006, arXiv:1506.07443.
[56] L.A. Harland-Lang, A.D. Martin, P. Motylinski, R.S. Thorne, Eur. Phys. J. C 75 (5) (2015) 204, arXiv:1412.3989.
[57] R.D. Ball, et al., NNPDF, J. High Energy Phys. 04 (2015) 040, arXiv:1410.8849.
[58] T.A. Aaltonen, et al., CDF, D0, Phys. Rev. Lett. 112 (2014) 231803, arXiv:1402.5126.
[59] K.G. Chetyrkin, J.H. Kühn, M. Steinhauser, Comput. Phys. Commun. 133 (2000) 43, arXiv:hep-ph/0004189.